Developmental presence and disappearance of postsynaptically silent synapses on dendritic spines of rat layer 2/3 pyramidal neurons

Giuseppe Busetto[1,2], Michael J. Higley[1] and Bernardo L. Sabatini[1]

[1] *Department of Neurobiology, Harvard Medical School, 220 Longwood Avenue, Boston, MA 02115, USA*
[2] *Dipartimento di Scienze Neurologiche e della Visione, Sezione di Fisiologia, Universita' di Verona, Strada le Grazie 8, 37134 Verona, Italy*

Silent synapses are synapses whose activation evokes NMDA-type glutamate receptor (NMDAR) but not AMPA-type glutamate receptor (AMPAR) mediated currents. Silent synapses are prominent early in postnatal development and are thought to play a role in the activity- and sensory-dependent refinement of neuronal circuits. The mechanisms that account for their silent nature have been controversial, and both presynaptic and postsynaptic mechanisms have been proposed. Here, we use two-photon laser uncaging of glutamate to directly activate glutamate receptors and measure AMPAR- and NMDAR-dependent currents on individual dendritic spines of rat somatosensory cortical layer 2/3 pyramidal neurons. We find that dendritic spines lacking functional surface AMPARs are commonly found before postnatal day 12 (P12) but are absent in older animals. Furthermore, AMPAR-lacking spines are contacted by release-competent presynaptic terminals. After P12, the AMPAR/NMDAR current ratio at individual spines continues to increase, consistent with continued addition of AMPARs to postsynaptic terminals. Our results confirm the existence of postsynaptically silent synapses and demonstrate that the morphology of the spine is not strongly predictive of its AMPAR content.

(Received 4 December 2007; accepted after revision 15 January 2008; first published online 17 January 2008)
Corresponding author B. L. Sabatini: Department of Neurobiology, Harvard Medical School, 220 Longwood Ave., Boston, MA 02115, USA. Email: bsabatini@hms.harvard.edu

In early postnatal life, many brain regions contain silent synapses whose activation does not result in a postsynaptic current when the neuron is at its resting potential (Isaac *et al.* 1995, 1997; Liao *et al.* 1995; Durand *et al.* 1996). Silent synapses can be converted into fully functional synapses by appropriate stimulation (Voronin & Cherubini, 2004), a process that may play a role in sensory-dependent circuit refinement and synaptic plasticity (Feldman & Brecht, 2005).

Silent synapses have been proposed to be synapses that express NMDARs but not AMPARs and thus, due to the Mg^{2+} block of NMDARs, do not generate appreciable synaptic currents at resting potentials. This hypothesis is supported by experiments using minimal stimulation (Isaac *et al.* 1995, 1997; Liao *et al.* 1995; Durand *et al.* 1996) and paired recordings (Montgomery *et al.* 2001) that describe synapses with only NMDAR-mediated responses that are revealed at depolarized potentials. Additional support comes from immunolabelling and ultrastructural studies that describe synapses devoid of AMPARs (Nusser *et al.* 1998; Liao *et al.* 1999; Petralia *et al.* 1999; Pickard *et al.* 2000; Washbourne *et al.* 2002). Furthermore, in visual cortex slices from newborn rats, NMDAR-mediated spontaneous miniature EPSCs (mEPSCs) occur at higher frequency than AMPAR-mediated mEPSCs (Rumpel *et al.* 2004). Moreoever, in hippocampal organotypic slice cultures, spines have been identified that display NMDAR-mediated Ca^{2+} transients without an associated synaptic potential (Ward *et al.* 2006).

An alternative hypothesis proposes that each postsynaptic terminal expresses both AMPARs and NMDARs and that silent synapses arise as a result of low glutamate concentration in the synaptic cleft that is only sufficient to activate NMDARs, which have higher glutamate affinity than AMPARs (Patneau & Mayer, 1990). Low glutamate concentration could result from impaired opening of vesicles into the synaptic cleft (Choi *et al.* 2000; Gasparini *et al.* 2000; Renger *et al.* 2001; Mozhayeva *et al.* 2002) or because glutamate diffuses into the cleft from a distant source (Kullmann *et al.* 1996; Gasparini *et al.* 2000). This hypothesis is supported by the findings that, in dissociated neurons, both AMPARs and NMDARs are found at newly formed synapses (Cottrell *et al.* 2000; Friedman *et al.*

This paper has online supplemental material.

 DOI: 10.1113/jphysiol.2007.149336

2000) and that, in hippocampal slices from newborn rats, AMPAR- and NMDAR-mediated spontaneous miniature EPSCs occur at similar frequencies (Groc *et al.* 2002).

Layer 2/3 pyramidal neurons in somatosensory cortex receive glutamatergic inputs from layer 4 neurons onto their basal dendrites (Lubke *et al.* 2000) and show synaptic refinement that is sensitive to whisker-based sensory exploration (Micheva & Beaulieu, 1996; Stern *et al.* 2001). In order to determine if postsynaptically silent synapses are formed onto these cells, we examined the AMPAR and NMDAR contents of basal dendritic spines in acute slices from P9–17 rats. Two-photon laser glutamate uncaging (2PLGU) was used to bypass the presynaptic terminal and directly activate glutamate receptors on each spine. We demonstrate the existence of AMPAR-lacking spines in animals younger than P12 that are morphologically indistinguishable from AMPAR-expressing ones. Moreover, AMPAR-lacking spines are associated with release-competent nerve terminals. Finally, the AMPAR content of individual spines continues to increase relative to the NMDAR content throughout the second and third postnatal week. Thus, our data directly demonstrate the existence of postsynaptically silent synapses formed onto basal dendrites of layer 2/3 neurons and indicate that the spine morphology is not strictly correlated with the maturational state of the associated synapse.

Methods

Slice preparation and electrophysiology

Animals were handled in accordance with Federal guidelines, and all protocols were approved by the animal welfare committee of Harvard Medical School. Sprague–Dawley rats were anaesthetized by inhalation of isofluorane and depth of anaesthesia was judged by lack of a righting reflex. Following decapitation, the cerebral hemispheres were quickly removed, placed in ice-cold dissection medium and reduced to blocks. The dissection medium consisted of (mM): 110 choline chloride, 25 $NaHCO_3$, 1.25 NaH_2PO_4, 2.5 KCl, 7 $MgCl_2$, 0.5 $CaCl_2$, 11.6 sodium ascorbate, 3.1 sodium pyruvate and 25 glucose, equilibrated with 95% O_2–5% CO_2. Coronal slices (300 μm thick) were cut from somatosensory cortex and collected in a holding chamber at 34°C for 30 min in artificial cerebrospinal fluid (ACSF) consisting of (mM): 127 NaCl, 25 $NaHCO_3$, 1.25 NaH_2PO_4, 2.5 KCl, 1 $MgCl_2$, 2 $CaCl_2$ and 25 glucose, equilibrated as above. Slices were subsequently transferred to a recording chamber perfused at 2 ml min^{-1} with ACSF at 22–25°C. The following drugs were dissolved in the ACSF (μM): 20 bicuculline (Tocris) and 50 picrotoxin (Tocris) to block $GABA_{A/C}$ receptors; 1 TTX to inhibit spontaneous activity; 100 LY341495 (Tocris) to block mGluRs; 10 serine to reduce NMDAR desensitization and fully occupy the glycine binding site; and 0.3 SNX-482 (Peptide Institute), 1 ω-conotoxin-MVIIC (Tocris), 10 mibefradil and 20 nimodipine (Tocris) to block R-, N/P/Q-, T- and L-type Ca^{2+} channels, respectively. These antagonists, in conjunction with intracellular Cs^+, improve voltage- and space-clamp and isolate synaptic signals mediated by AMPARs and NMDARs. To monitor uncaging-evoked excitatory postsynaptic currents (uEPSCs) mediated by AMPARs and NMDARs ($uEPSC_{AMPAR}$ and $uEPSC_{NMDAR}$, respectively), 2.5 or 5.0 mM 4-methoxy-7-nitroindolinyl-caged L-glutamate (MNI-glutamate; Tocris) was dissolved in the ACSF. When appropriate, AMPARs or NMDARs were blocked with 10 μM NBQX or (±)-3-(2-carboxypiperazin-4-yl)-propyl-1-phosphonic acid (CPP), respectively.

Whole-cell voltage-clamp recordings (Multiclamp 700A, Axon Instruments) were obtained from layer 2/3 pyramidal neurons (soma to pial surface distance: ~300 μm; range: 162–511 μm) visualized with infrared differential interference contrast optics and recognized as pyramidal neurons by their morphology under two-photon laser scanning microscopy (2PLSM; see below). Cells were voltage clamped at −70 or +40 mV to monitor $uEPSC_{AMPAR}$ or $uEPSC_{NMDAR}$, respectively. Recording electrodes (3–5 MΩ) were made with borosilicate glass (Warner Instruments) and filled with (mM): 135 caesium methanesulphonate, 10 Hepes, 10 sodium phosphocreatine, 4 $MgCl_2$, 4 Na-ATP, 0.4 Na-GTP, pH 7.4 with CsOH. The intracellular solution contained the red fluorophore Alexa Fluor-594 (20 μM, Molecular Probes) to visualize the cell morphology, and the green-fluorescing Ca^{2+} indicator Fluo-5F (300 or 500 μM, Molecular Probes) to detect intracellular Ca^{2+} transients. All drugs were obtained from Sigma except when otherwise indicated. Currents were filtered at 2 kHz and digitized at 10 kHz. Series resistance (< 20 MΩ in all analysed recordings) and whole-cell capacitance were not compensated.

Imaging and uncaging

Two-photon laser scanning microscopy (2PLSM) and 2PLGU were performed using a custom microscope (Carter & Sabatini, 2004; Bloodgood & Sabatini, 2007). The laser for 2PLSM was tuned to 840 nm to excite both red and green fluorophores. This wavelength does not cause photolysis of the MNI-glutamate, as judged by the absence of NMDAR-mediated Ca^{2+} transients in spines of neurons held at 0 mV potential and visualized with 2PLSM at different wavelengths within the 810–860 nm range (data not shown). Spine morphology was measured from maximal projections of 3-dimensional image stacks

(5–6 sections at 1.0 μm spacing, 256 × 256 resolution, image field of 7.6 × 7.6 μm). Spine length was measured from the junction with the dendritic shaft to the spine tip. To determine the apparent spine width, we measured fluorescence in a line across the head and determined the width of the distribution where fluorescence intensity fell to 50% of its maximum. This measurement is an overestimate of the true spine head width as it includes the distortion caused by the point-spread function of the microscope. To minimize voltage-clamp errors, spines located close to the soma (range 16–89 μm) were analysed.

Fluorescence transients were monitored in line (500 Hz) or frame (4Hz) scans, and quantified as increases in green fluorescence divided by red fluorescence ($\Delta G/R$) (Sabatini *et al.* 2002). Application of hypertonic ACSF (500 mosmol l^{-1} by sucrose addition) was accomplished by puffing onto the surface of the slice through a syringe connected to a pipette whose 5–10 μm tip was positioned above the spine of interest.

2PLGU was achieved by dissolving 2.5 or 5.0 mM MNI-glutamate in the bath and triggered by 0.3–0.8 ms (typically 0.5 ms) pulses of 720 nm laser light. For each spine, we determined the 'best spot' of uncaging around the spine head by systematically testing uncaging positions around the periphery of the spine head and finding the one where 2PLGU elicited the biggest uEPSC at −70 mV (Fig. 1*B*). Repeated uncaging at this spot was ensured using a stabilization routine that cancelled image drift during the interstimulus interval (Carter & Sabatini, 2004). uEPSC amplitude was measured at each potential from the average of 10 uncaging trials, delivered at 0.033 Hz. Spines whose $uEPSC_{AMPAR}$ amplitude was less than 2 standard deviations of the current during a 5 ms period before the stimulus were defined as silent.

Data are presented as means ± standard error of the mean. Student's two tail *t* test was used ($P < 0.05$) to judge statistical significance.

Results

Whole-cell voltage-clamp recordings of pyramidal neurons were obtained in cortical slices of 2-week-old rats (P14–17). Neurons were filled with the red fluorophore Alexa Fluor-594 (Fig. 1*A*). Dendrites and spines were visualized with two-photon laser scanning microscopy (2PLSM) and brief pulses of 720 nm light were used to trigger two-photon laser glutamate uncaging (2PLGU). The uncaging laser beam was directed at the position on the periphery of the selected spine head that evoked the largest response. The evoked currents at this optimal location were ∼2- to 3-fold larger than those evoked at the diametrically opposed spot, relative to the spine head (Fig. 1*B* and *C*). This strong location dependence is consistent with the high spatial resolution of 2PLGU and suggests direct stimulation of synaptic AMPARs (Matsuzaki *et al.* 2001; Sobczyk *et al.* 2005; Carter *et al.* 2007). By bypassing the presynaptic terminal, we avoid complications of the presence of presynaptically silent synapses and of changes in the probability of vesicular release or quantal content during development. We focused on spines of basal dendrites, the main site of innervation by excitatory inputs from neurons located in cortical layer 4 (Lubke *et al.* 2000). Furthermore, we only considered spines whose head was clearly wider than the spine neck, and we refer to such spines as 'morphologically mature' below. We did not examine structures with no discernible head that might have represented either filopodia or long spines with small heads.

At a holding potential of −70 mV, uEPSCs were inward, short-lived (Fig. 1*D*), and suppressed by the

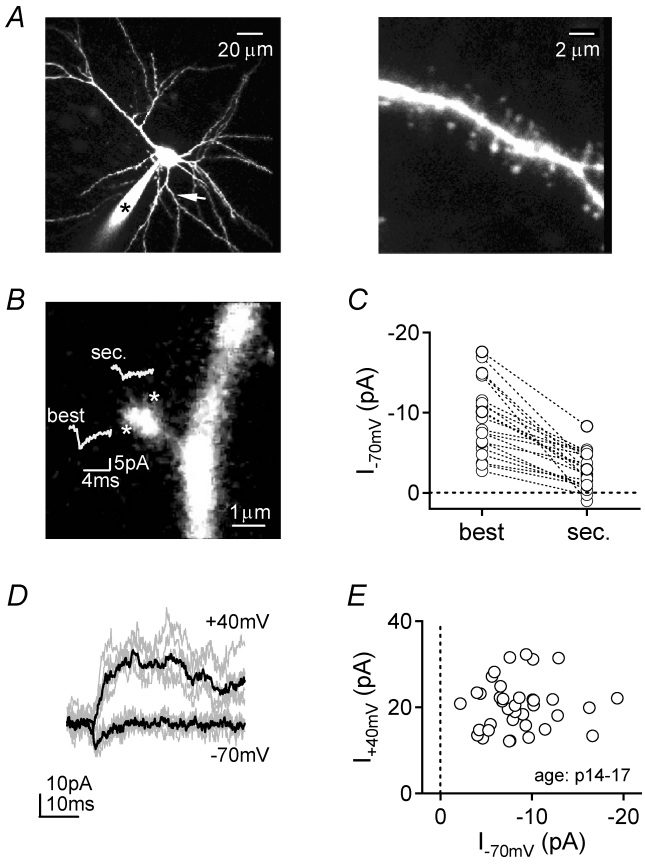

Figure 1. 2PLGU selectively activates individual dendritic spines
A, left panel, image of a layer 2/3 pyramidal neuron from a P16 rat. The asterisk and arrow highlight, respectively, the recording electrode and the spiny basal dendrite shown at higher magnification in the right panel. *B*, image of a spine and its parent dendrite. Asterisks indicate uncaging locations that yielded the largest ('best') and a secondary ('sec.') uEPSCs. The insets show the average $uEPSC_{AMPAR}$ at each spot. *C*, $uEPSC_{AMPAR}$ from 'best' and 'secondary' spots in 21 spines. *D*, uEPSCs from a P16 spine at holding potentials of −70 and +40 mV; 5 individual trials (grey) and the corresponding averages (black) are shown. *E*, $uEPSC_{NMDAR}$ from individual dendritic spines of P14–17 animals plotted *versus* $uEPSC_{AMPAR}$ ($n = 37$ spines).

application of 10 μM NBQX in the bath (Fig. 2*C*). For these reasons, they were consistent with activation of AMPARs. Depolarization to +40 mV revealed the presence of long-lived outward currents (Fig. 1*D*) whose slowly decaying component was suppressed by 10 μM CPP (Fig. 4*B*) and thus were consistent with the activation of NMDARs. The average current amplitude at −70 mV in a 2 ms window about the peak was used to quantify $uEPSC_{AMPAR}$. The average amplitude of the current at +40 mV during a 20–40 ms window after the uncaging pulse was used to quantify $uEPSC_{NMDAR}$. In a separate set of spines, the dependence of $uEPSC_{NMDAR}$ on the uncaging position was determined (online supplemental material, Supplemental Fig. 1). In 5 of 7 spines, the location that produced the largest $uEPSC_{NMDAR}$ coincided with that which produced the largest $uEPSC_{AMPAR}$. In the remaining two spines, uncaging at the spot that was optimal for $uEPSC_{AMPAR}$ evoked current at +40 mV that was at least 75% of the maximal $uEPSC_{NMDAR}$. These results are consistent with the low dependence of NMDAR activation of the location of the uncaging spot (Noguchi *et al.* 2005; Sobczyk *et al.* 2005; Carter *et al.* 2007).

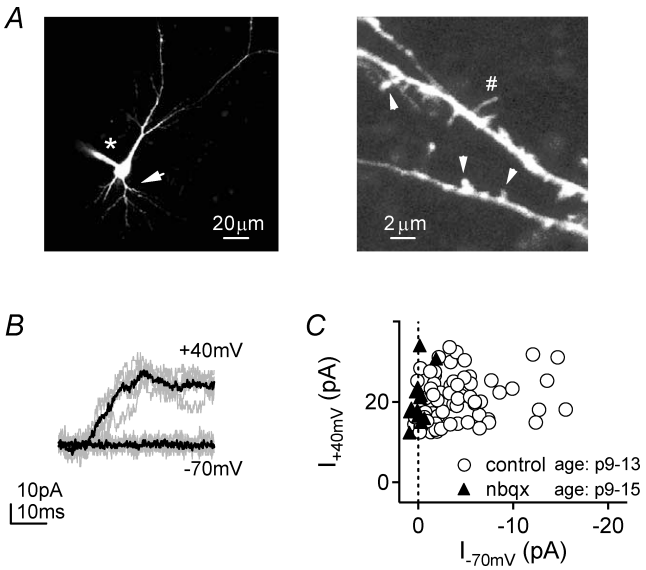

Figure 2. AMPAR-lacking spines are found in immature pyramidal neurons
A, left panel, image of a layer 2/3 pyramidal neuron from a P9 rat highlighting the recording electrode (*). Right panel, higher magnification image of the basal dendrite indicated by the arrow in the left panel, showing mature spines (arrowheads) and a filopodium (#). *B*, uEPSCs from a P9 spine at holding potentials of −70 and +40 mV; 5 individual trials (grey) and the corresponding averages (black) are shown. *C*, $uEPSC_{NMDAR}$ plotted *versus* $uEPSC_{AMPAR}$ in control conditions (○, $n = 72$ spines, P9–13) or in the presence of NBQX (▲, $n = 13$ spines, P9–15). The dashed line marks the position expected for spines lacking AMPARs. Many control spines fall along this line and show $uEPSC_{AMPAR}$ similar to that recorded in the presence of NBQX.

In order to compare $uEPSC_{AMPAR}/uEPSC_{NMDAR}$ ratios across cells and development, the laser power was set to obtain a ∼20 pA $uEPSC_{NMDAR}$ when uncaging at the optimal spot determined at −70 mV (on average $uEPSC_{NMDAR} = 20.4 \pm 0.94$ pA, $n = 37/28/15$ spines/cells/animals, age P14–17). This large amplitude $uEPSC_{NMDAR}$ at +40 mV was chosen to ensure that the level of glutamate released by the uncaging pulse was sufficient to activate AMPARs on the spine. At P14–17, every analysed spine showed clear $uEPSC_{AMPAR}$ (on average -8.5 ± 0.61 pA) (Fig. 1*E*), indicating surface expression of AMPARs and NMDARs at each spine (Kharazia *et al.* 1996; Takumi *et al.* 1999) and consistent with reports of low silent synapse density at these ages (Durand *et al.* 1996; Isaac *et al.* 1997; Rumpel *et al.* 2004). Furthermore, this uEPSC amplitude is similar to that of spontaneous miniature EPSCs at −70 mV in layer 2/3 pyramidal neurons of P11–22 rat somatosensory cortex (Bender *et al.* 2006).

AMPAR-lacking, morphologically mature spines in immature rats

In spines from rats younger than 2 weeks (P9–13), $uEPSC_{NMDAR}$ of similar amplitude (average 20.6 ± 0.67 pA, $n = 72/52/27$ spines/cells/animals) and time course (Supplemental Fig. 2) to that in older animals was obtained. However, spines could be identified that demonstrated uEPSCs at +40 mV but not at −70 mV (Fig. 2*B* and *C*). In these spines, $uEPSC_{AMPAR}$ (on average -0.4 ± 0.10 pA, $n = 15/14/11$ spines/cells/animals) was similar to that seen in the presence of the AMPAR antagonist NBQX (on average -0.1 ± 0.20 pA, $n = 13/5/3$ spines/cells/animals; $P > 0.1$), consistent with a lack of functional surface AMPARs. Furthermore, $uEPSC_{AMPAR}$ averaged across all spines (-3.9 ± 0.45 pA) and across only non-silent spines (-4.9 ± 0.49 pA, $n = 57/38/16$ spines/cells/animals) from P9–13 animals were significantly decreased compared to data from P14–17 animals. To confirm that spines of similar morphology had been analysed across ages, we measured the apparent length and head-width of spines in the study (Fig. 3). These parameters were constant across the age range (Fig. 3*B*), confirming that the increase in $uEPSC_{AMPAR}$ reflected developmental changes. Furthermore, no significant correlations were observed between $uEPSC_{AMPAR}$ and spine length (Fig. 3*C*, $R^2 = 0.08$) or width ($R^2 = 0.04$, data not shown).

Despite nearly constant morphology of analysed spines, AMPAR-lacking spines were found only in young animals. Thus, the percentage of spines with $uEPSC_{AMPAR}$ indistinguishable from noise was 39% at P9, 32% at P10, 7% at P11 and 0% in older animals (Fig. 3*D*). Moreover, $uEPSC_{AMPAR}$ increased consistently with age,

including during the week following the disappearance of AMPAR-lacking spines (Fig. 3*E*). This is consistent with the described increase in AMPAR/NMDAR synaptic current ratios in the same neurons early in development (Mierau *et al.* 2004).

Silent spines are associated with release-competent presynaptic terminals

2PLGU probes the glutamate receptor content of individual spines but cannot confirm the presence of a functional synapse, which requires a competent presynaptic terminal. To determine if an individual spine analysed by 2PLGU was associated with a release-competent presynaptic terminal, we used puffs of hypertonic solution to evoke the release of the readily releasable pool of glutamatergic vesicles (Fig. 4). In young animals, the mEPSC rate is low and the holding current at −70 mV shows small fluctuations. In contrast, during application of hypertonic ACSF, the mEPSC rate and holding current fluctuations are greatly increased (Fig. 4*A*). To detect glutamate release from the presynaptic terminal onto the analysed spine, the green-fluorescing Ca^{2+} indicator Fluo-5F was included in the recording pipette, and Ca^{2+} transients in the spine head were monitored during application of hypertonic solution. In order to minimize movement of the imaged spine during puffing, the hypertonic solution was applied to the surface of the slice, resulting in activation of only a single or few spines within the field of view (Supplemental Fig. 3).

Individual spines were first analysed electrophysiologically as above using 2PLGU (Fig. 4*B*), and $uEPSC_{AMPAR}$ and $uEPSC_{NMDAR}$ were measured. The cell was subsequently held at 0 mV, and a line scan was performed across the spine head and parent dendrite while puffing the hypertonic solution. In a subset of spines, Ca^{2+} transients were seen in the spine head during the puff that were absent in the adjacent dendrite (Fig. 4*C* and *D*). These transients were blocked by CPP (Fig. 4*D*), together with $uEPSC_{NMDAR}$ (Fig. 4*B*), and were consistent with the known time course and spatial confinement of synaptically evoked NMDAR-mediated Ca^{2+} transients in active spines (Sabatini *et al.* 2002; Carter & Sabatini, 2004). Similar Ca^{2+} transients were seen in ∼50% of spines, indicating that they were associated with a release-competent terminal. Ca^{2+} transients were detected in both AMPAR-expressing and AMPAR-lacking spines, supporting the notion that the latter represent the postsynaptic component of postsynaptically silent synapses (Fig. 4*E*). Spines that did not respond to hypertonic puffs may not have been exposed to effective levels of sucrose or they may represent spines not associated with release-competent terminals.

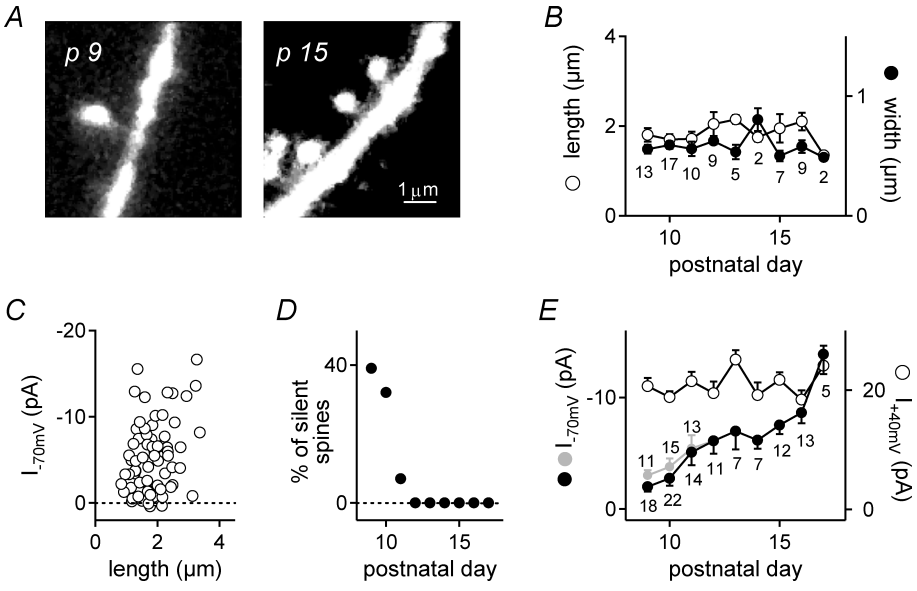

Figure 3. Spines lacking or expressing AMPARs are morphologically indistinguishable
A, images of spines from relatively immature (left panel) and mature (right panel) rats. *B*, mean length (○, left ordinate) and width (●, right ordinate) of spines analysed electrophysiologically as a function of animal age. The numbers of analysed spines at each age are indicated. *C*, $uEPSC_{AMPAR}$ plotted *versus* spine length ($n = 74$ spines). Dashed line marks the predicted position of AMPAR-lacking spines. *D*, percentage of AMPAR-lacking spines as a function of animal age. *E*, developmental curve of $uEPSC_{AMPAR}$ (●) and $uEPSC_{NMDAR}$ (○). The average uEPSCs calculated from the subset of spines that are non-silent in P9–11 animals are shown by grey circles. The numbers of analysed spines contributing to each data point are also given.

Discussion

We used a combination of 2PLSM, 2PLGU and whole-cell recordings to examine AMPAR- and NMDAR-mediated currents at single spines during development. We examined layer 2/3 pyramidal neurons in acute slices of rat somatosensory cortex and focused on spines of basal dendrites, which receive glutamatergic inputs from layer 4. Our results demonstrate the existence of postsynaptically silent synapses and show that, before age P12, these synapses can be found on morphologically mature spines. At later ages, all studied spines had functional surface AMPARs, but the AMPAR/NMDAR current ratio at individual spines continued to increase with age, consistent with increased synaptic expression of AMPARs.

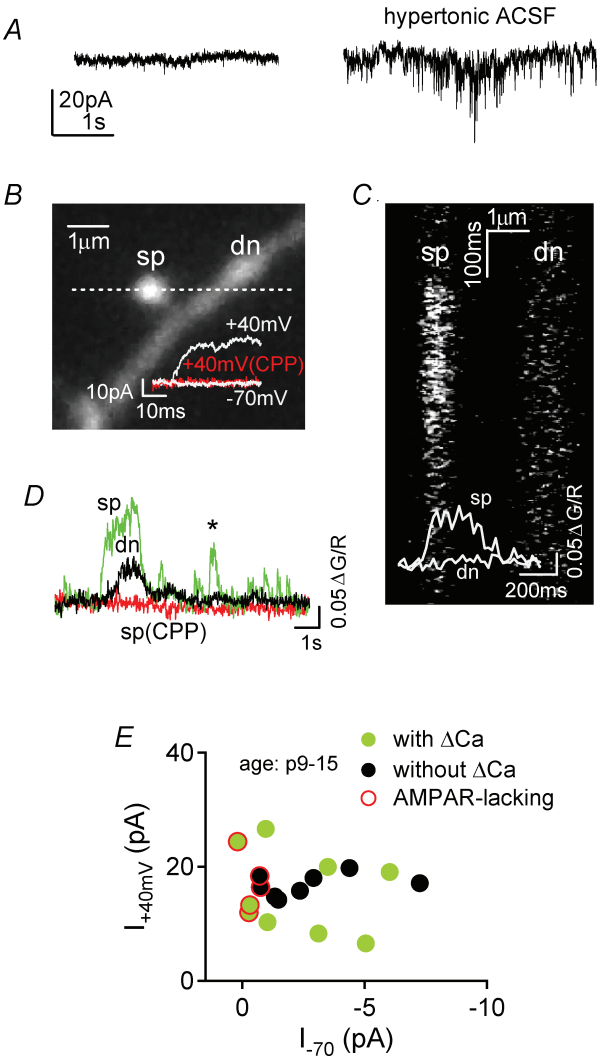

Figure 4. Spines lacking AMPARs are associated with functional presynaptic terminals
A, the rate of mEPSCs detected at −70 mV is increased by puffs of hypertonic solution (right panel) relative to baseline levels (left panel) (age P9). *B*, image of a parent dendrite (dn) and spine (sp.) that showed no uEPSCs at −70 mV and large currents at +40 mV (white traces) that are blocked by the NMDAR antagonist CPP (red trace) (age P10). *C*, green fluorescence collected in the line scan indicated by the dashed line in (*B*). Inset: quantification of the green fluorescence transient ($\Delta G/R$) in the spine head (sp) and neighbouring dendrite (dn) indicating that Ca^{2+} influx was limited to the spine. *D*, quantification of fluorescence transients in the spine (sp, green trace) and dendrite (dn, black trace) on a longer time scale than *C*, displaying several evoked Ca^{2+} transients in the spine. Over this longer time scale, evidence of Ca^{2+} diffusion in the parent dendrite is seen. The asterisk (*) marks the event shown in (*C*). Ca^{2+} influx into the spine was blocked by CPP (red trace). *E*, $uEPSC_{NMDAR}$ plotted *versus* $uEPSC_{AMPAR}$ for spines that were exposed to hypertonic ACSF. In some cases a Ca^{2+} increase restricted to the spine was evoked (green circle, $n = 9$), whereas in others ΔCa^{2+} was not detectable or was not restricted to the spine (●, $n = 8$) (age P9–15). A red contour marks AMPAR-lacking spines.

Postsynaptic nature of silent synapses

Silent synapses were initially described as synapses that display currents at +40 mV but not at −70 mV and were interpreted as containing NMDARs but lacking AMPARs (Isaac *et al.* 1995; Liao *et al.* 1995; Durand *et al.* 1996; Montgomery *et al.* 2001). However, other studies suggested that silent synapses might reflect synapses exposed to low levels of glutamate that are sufficient to activate NMDARs but not the lower affinity AMPARs. The postsynaptic terminals of silent synapses might be exposed to a reduced level of glutamate released by a competent nerve terminal (Choi *et al.* 2000; Renger *et al.* 2001; Mozhayeva *et al.* 2002) or to glutamate that enters the cleft due to spillover from neighbouring synapses (Kullmann *et al.* 1996; Gasparini *et al.* 2000).

2PLGU bypasses the presynaptic terminal and, when used to stimulate spines longer than ∼1 μm, allows the selective activation of the postsynaptic terminal of a single spine (Matsuzaki *et al.* 2001; Sabatini *et al.* 2002; Carter & Sabatini, 2004; Beique *et al.* 2006). The dependence of uEPSC amplitudes on the location of the uncaging spot (Fig. 1*B* and *C*) suggests that a highly localized group of receptors is activated, such as that associated with the postsynaptic-density. Nevertheless, the volume in which glutamate is released is larger than that of the synaptic cleft, and extrasynaptic glutamate receptors are undoubtedly stimulated. Thus, spines without $uEPSC_{AMPAR}$ lack functional surface AMPARs both in the synapse and in the perisynaptic membrane. These spines may lack surface AMPARs or may express a nonfunctional or silenced receptor (Xiao *et al.* 2004).

Our results indicate that AMPAR-lacking spines are found in young animals (Fig. 2) and that NMDARs located on these spines detect glutamate released from presynaptic terminals (Fig. 4). Thus, we conclude that postsynaptically silent synapses do exist and, in basal dendrites of layer 2/3 pyramidal neurons, are associated with morphologically mature dendritic spines. Nevertheless, it is impossible to disprove that the glutamate which activates NMDARs on the AMPAR-lacking spines diffuses ('spillover') from a neighbouring synapse. The degree of spillover may have

been enhanced in our experiments, which were performed at room temperature (Asztely *et al.* 1997). Lastly, we cannot rule out that presynaptically silent synapses also exist, and it is possible that some of the AMPAR-lacking spines that could not be stimulated by hypertonic sucrose puffs represent the postsynaptic component of such synapses.

Development of layer 2/3 synapses

As has been previously described for silent synapses (Durand *et al.* 1996; Isaac *et al.* 1997), we find that AMPAR-lacking spines are present in developing animals and disappear (or become extremely rare) by age P12 (Fig. 3*D*). Rumpell and colleagues examined the development of silent synapses in layer 2/3 pyramidal neurons of the visual cortex and found them to be present until P14 (Rumpel *et al.* 2004). The two findings are in general good agreement; the slightly longer time of expression of silent synapses in the Rumpell paper may arise from experimental differences such as the activation of apical and basal synapses in their study and differences between visual and somatosensory cortex. Furthermore, the silent synapses found by Rumpel and colleagues may include synapses made onto filopodia or directly onto the dendritic shaft, classes of synapses that we did not examine. Lastly, the spines that we describe as lacking AMPARs lack them in the postsynaptic density and are therefore silent. However, the converse may not be true: it is possible that some spines that have functional surface AMPARs may lack them in the synaptic cleft and be silent when exposed to synaptically released glutamate. For all of these reasons, the fraction of spines that lack uncaging-evoked AMPARs currents is likely an underestimate of the fraction of synapses that are silent.

Our results also show that the transition from silent to non-silent during development does not involve a binary, step-like increase in AMPAR content. Before P12, the size of $uEPSC_{AMPAR}$ in spines that show such currents is small with many responses clustered below 5 pA (Fig. 2*C*). AMPAR content increases with age, including after age P12 when silent spines are no longer found (Fig. 3*E*). Similar increases in synaptically evoked AMPAR/NMDAR current ratios have been described in layer 2/3 somatosensory cortical neurons (Mierau *et al.* 2004) and may account for their weak response to whisker stimulation before P14 (Stern *et al.* 2001). Gradual AMPAR expression, in addition to an increased number of synapses, may contribute to the strengthening input/output relation seen in hippocampal CA3–CA1 connections during development (Hsia *et al.* 1998).

During the developmental time period investigated in the present paper, NMDAR subunit composition changes (Carmignoto & Vicini, 1992) from a subtype containing predominantly NR1/NR2B subunits to a subtype containing NR1/NR2A/NR2B in variable combinations (Sheng *et al.* 1994). Decreasing contribution of NR2B subunit during the second postnatal week has been demonstrated in layer 2/3 pyramidal neurons of somatosensory cortex (Mierau *et al.* 2004). Notwithstanding the shift in subunit composition, the unitary current amplitudes of recombinant NR1/NR2A and NR1/NR2B channels are the same (Stern *et al.* 1992; Cull-Candy *et al.* 2001) in the presence of 10 μM glycine (replaced here with 10 μM of its analogue serine). An additional complication of the NR2B to NR2A subtype switch is that the opening probability of recombinant NR2A containing receptors is higher than those containing NR2B (Chen *et al.* 1999; Erreger *et al.* 2005) (although see Prybylowski *et al.* (2002), who report that the opening probability of NMDARs does not differ depending on the NR2 subunit that is incorporated). For this reason it is possible that less uncaged glutamate was needed to produce a 20 pA uEPSC in old animals than in young animals. If this case, we may have underestimated the AMPAR/NMDAR current ratio in older animals as well as the rate of increase of this ratio during development.

Spine morphology

The definition of a silent synapse is strictly functional. A recent study performed in organotypic hippocampal slice cultures has visualized the dendritic spines associated with silent synapses (Ward *et al.* 2006). The authors discuss that those silent spines were 'no different in appearance' from the active ones, although no supporting data were given. In accordance with this paper, we find that both AMPAR-lacking and AMPAR-containing spines are found within the class of morphologically mature spines. Similarly, 2PLGU analysis of single spines of CA1 pyramidal neurons of PSD-95 knock-out mice uncovered a high percentage of AMPAR-lacking spines that were morphologically similar to spines with AMPARs (Beique *et al.* 2006). In the same report, no postsynaptically silent spines were found in age-matched (P13–16) control animals. In separate studies, hippocampal spines immunonegative for AMPARs have been shown to have smaller synaptic area than spines with synaptic AMPARs (Nusser *et al.* 1998; Takumi *et al.* 1999). Similarly, 2PLGU analysis of single hippocampal spines in P15–22 animals demonstrated a tight correlation between AMPAR-current amplitude and spine morphology such that small or thin structures had little sensitivity to glutamate (Matsuzaki *et al.* 2001). In the present paper, we found a large variability in AMPAR-current amplitudes within a relatively morphologically homogeneous population of spines. Our study examined only spines with clear necks and heads. Therefore, the results may not be applicable to small spines that are below the resolution of 2PLSM or to stubby spines that, because of their short length, cannot be

selectively activated by glutamate uncaging without also activating glutamate receptors located on the dendritic shaft.

Conclusion

We used combined two-photon microscopy and glutamate uncaging to directly demonstrate the existence of dendritic spines on basal dendrites of layer 2/3 pyramidal neurons that express functional NMDARs but not AMPARs. At least a subset of these AMPAR-lacking spines is associated with release competent presynaptic boutons, indicating the existence of postsynaptically silent synapses. Furthermore, AMPAR-lacking spines on these cells were found only prior to P12, and the AMPAR/NMDAR current ratio at individual spines continued to increase through the following postnatal week.

References

Asztely F, Erdemli G & Kullmann DM (1997). Extrasynaptic glutamate spillover in the hippocampus: dependence on temperature and the role of active glutamate uptake. *Neuron* **18**, 281–293.

Beique JC, Lin DT, Kang MG, Aizawa H, Takamiya K & Huganir RL (2006). Synapse-specific regulation of AMPA receptor function by PSD-95. *Proc Natl Acad Sci U S A* **103**, 19535–19540.

Bender KJ, Allen CB, Bender VA & Feldman DE (2006). Synaptic basis for whisker deprivation-induced synaptic depression in rat somatosensory cortex. *J Neurosci* **26**, 4155–4165.

Bloodgood BL & Sabatini BL (2007). Nonlinear regulation of unitary synaptic signals by $Ca_V2.3$ voltage-sensitive calcium channels located in dendritic spines. *Neuron* **53**, 249–260.

Carmignoto G & Vicini S (1992). Activity-dependent decrease in NMDA receptor responses during development of the visual cortex. *Science* **258**, 1007–1011.

Carter AG & Sabatini BL (2004). State-dependent calcium signaling in dendritic spines of striatal medium spiny neurons. *Neuron* **44**, 483–493.

Carter AG, Soler-Llavina GJ & Sabatini BL (2007). Timing and location of synaptic inputs determine modes of subthreshold integration in striatal medium spiny neurons. *J Neurosci* **27**, 8967–8977.

Chen N, Luo T & Raymond LA (1999). Subtype-dependence of NMDA receptor channel open probability. *J Neurosci* **19**, 6844–6854.

Choi S, Klingauf J & Tsien RW (2000). Postfusional regulation of cleft glutamate concentration during LTP at 'silent synapses'. *Nat Neurosci* **3**, 330–336.

Cottrell JR, Dube GR, Egles C & Liu G (2000). Distribution, density, and clustering of functional glutamate receptors before and after synaptogenesis in hippocampal neurons. *J Neurophysiol* **84**, 1573–1587.

Cull-Candy S, Brickley S & Farrant M (2001). NMDA receptor subunits: diversity, development and disease. *Curr Opin Neurobiol* **11**, 327–335.

Durand GM, Kovalchuk Y & Konnerth A (1996). Long-term potentiation and functional synapse induction in developing hippocampus. *Nature* **381**, 71–75.

Erreger K, Dravid SM, Banke TG, Wyllie DJ & Traynelis SF (2005). Subunit-specific gating controls rat NR1/NR2A and NR1/NR2B NMDA channel kinetics and synaptic signalling profiles. *J Physiol* **563**, 345–358.

Feldman DE & Brecht M (2005). Map plasticity in somatosensory cortex. *Science* **310**, 810–815.

Friedman HV, Bresler T, Garner CC & Ziv NE (2000). Assembly of new individual excitatory synapses: time course and temporal order of synaptic molecule recruitment. *Neuron* **27**, 57–69.

Gasparini S, Saviane C, Voronin LL & Cherubini E (2000). Silent synapses in the developing hippocampus: lack of functional AMPA receptors or low probability of glutamate release? *Proc Natl Acad Sci U S A* **97**, 9741–9746.

Groc L, Gustafsson B & Hanse E (2002). Spontaneous unitary synaptic activity in CA1 pyramidal neurons during early postnatal development: constant contribution of AMPA and NMDA receptors. *J Neurosci* **22**, 5552–5562.

Hsia AY, Malenka RC & Nicoll RA (1998). Development of excitatory circuitry in the hippocampus. *J Neurophysiol* **79**, 2013–2024.

Isaac JT, Crair MC, Nicoll RA & Malenka RC (1997). Silent synapses during development of thalamocortical inputs. *Neuron* **18**, 269–280.

Isaac JT, Nicoll RA & Malenka RC (1995). Evidence for silent synapses: implications for the expression of LTP. *Neuron* **15**, 427–434.

Kharazia VN, Phend KD, Rustioni A & Weinberg RJ (1996). EM colocalization of AMPA and NMDA receptor subunits at synapses in rat cerebral cortex. *Neuroscience Letters* **210**, 37–40.

Kullmann DM, Erdemli G & Asztely F (1996). LTP of AMPA and NMDA receptor-mediated signals: evidence for presynaptic expression and extrasynaptic glutamate spill-over. *Neuron* **17**, 461–474.

Liao D, Hessler NA & Malinow R (1995). Activation of postsynaptically silent synapses during pairing-induced LTP in CA1 region of hippocampal slice. *Nature* **375**, 400–404.

Liao D, Zhang X, O'Brien R, Ehlers MD & Huganir RL (1999). Regulation of morphological postsynaptic silent synapses in developing hippocampal neurons. *Nat Neurosci* **2**, 37–43.

Lubke J, Egger V, Sakmann B & Feldmeyer D (2000). Columnar organization of dendrites and axons of single and synaptically coupled excitatory spiny neurons in layer 4 of the rat barrel cortex. *J Neurosci* **20**, 5300–5311.

Matsuzaki M, Ellis-Davies GC, Nemoto T, Miyashita Y, Iino M & Kasai H (2001). Dendritic spine geometry is critical for AMPA receptor expression in hippocampal CA1 pyramidal neurons. *Nat Neurosci* **4**, 1086–1092.

Micheva KD & Beaulieu C (1996). Quantitative aspects of synaptogenesis in the rat barrel field cortex with special reference to GABA circuitry. *J Comp Neurol* **373**, 340–354.

Mierau SB, Meredith RM, Upton AL & Paulsen O (2004). Dissociation of experience-dependent and -independent changes in excitatory synaptic transmission during development of barrel cortex. *Proc Natl Acad Sci U S A* **101**, 15518–15523.

Montgomery JM, Pavlidis P & Madison DV (2001). Pair recordings reveal all-silent synaptic connections and the postsynaptic expression of long-term potentiation. *Neuron* **29**, 691–701.

Mozhayeva MG, Sara Y, Liu X & Kavalali ET (2002). Development of vesicle pools during maturation of hippocampal synapses. *J Neurosci* **22**, 654–665.

Noguchi J, Matsuzaki M, Ellis-Davies GC & Kasai H (2005). Spine-neck geometry determines NMDA receptor-dependent Ca^{2+} signaling in dendrites. *Neuron* **46**, 609–622.

Nusser Z, Lujan R, Laube G, Roberts JD, Molnar E & Somogyi P (1998). Cell type and pathway dependence of synaptic AMPA receptor number and variability in the hippocampus. *Neuron* **21**, 545–559.

Patneau DK & Mayer ML (1990). Structure-activity relationships for amino acid transmitter candidates acting at *N*-methyl-D-aspartate and quisqualate receptors. *J Neurosci* **10**, 2385–2399.

Petralia RS, Esteban JA, Wang YX, Partridge JG, Zhao HM, Wenthold RJ & Malinow R (1999). Selective acquisition of AMPA receptors over postnatal development suggests a molecular basis for silent synapses. *Nat Neurosci* **2**, 31–36.

Pickard L, Noel J, Henley JM, Collingridge GL & Molnar E (2000). Developmental changes in synaptic AMPA and NMDA receptor distribution and AMPA receptor subunit composition in living hippocampal neurons. *J Neurosci* **20**, 7922–7931.

Prybylowski K, Fu Z, Losi G, Hawkins LM, Luo J, Chang K, Wenthold RJ & Vicini S (2002). Relationship between availability of NMDA receptor subunits and their expression at the synapse. *J Neurosci* **22**, 8902–8910.

Renger JJ, Egles C & Liu G (2001). A developmental switch in neurotransmitter flux enhances synaptic efficacy by affecting AMPA receptor activation. *Neuron* **29**, 469–484.

Rumpel S, Kattenstroth G & Gottmann K (2004). Silent synapses in the immature visual cortex: layer-specific developmental regulation. *J Neurophysiol* **91**, 1097–1101.

Sabatini BL, Oertner TG & Svoboda K (2002). The life cycle of Ca^{2+} ions in dendritic spines. *Neuron* **33**, 439–452.

Sheng M, Cummings J, Roldan LA, Jan YN & Jan LY (1994). Changing subunit composition of heteromeric NMDA receptors during development of rat cortex. *Nature* **368**, 144–147.

Sobczyk A, Scheuss V & Svoboda K (2005). NMDA receptor subunit-dependent $[Ca^{2+}]$ signaling in individual hippocampal dendritic spines. *J Neurosci* **25**, 6037–6046.

Stern P, Behe P, Schoepfer R & Colquhoun D (1992). Single-channel conductances of NMDA receptors expressed from cloned cDNAs: Comparison with native receptors. *Proc Biol Sci* **250**, 271–277.

Stern E, Maravall M & Svoboda K (2001). Rapid development and plasticity of layer 2/3 maps in rat barrel cortex in vivo. *Neuron* **31**, 305–315.

Takumi Y, Ramirez-Leon V, Laake P, Rinvik E & Ottersen OP (1999). Different modes of expression of AMPA and NMDA receptors in hippocampal synapses. *Nat Neurosci* **2**, 618–624.

Voronin LL & Cherubini E (2004). 'Deaf, mute and whispering' silent synapses: their role in synaptic plasticity. *J Physiol* **557**, 3–12.

Ward B, McGuinness L, Akerman CJ, Fine A, Bliss TV & Emptage NJ (2006). State-dependent mechanisms of LTP expression revealed by optical quantal analysis. *Neuron* **52**, 649–661.

Washbourne P, Bennett JE & McAllister AK (2002). Rapid recruitment NMDA receptor transport packets to nascent synapses. *Nat Neurosci* **5**, 751–759.

Xiao MY, Wasling P, Hanse E & Gustafsson B (2004). Creation of AMPA-silent synapses in the neonatal hippocampus. *Nat Neurosci* **7**, 236–243.

Acknowledgements

We thank members of the Sabatini lab for useful comments and critical reading of the manuscript. This work was funded by the McKnight and Searle Foundations, the National Institutes of Neurological Disorders and Stroke (RO1 NS046579), and National Institutes of Health Training Grant 5T32 NS07484 (M.J.H.).

Supplemental material

Online supplemental material for this paper can be accessed at:
http://jp.physoc.org/cgi/content/full/jphysiol.2007.149336/DC1
and
http://www.blackwell-synergy.com/doi/suppl/10.1113/jphysiol.2007.149336